Energy and temperature dependence of relaxation time and Wiedemann-Franz law on PbTe

Salameh Ahmad and S. D. Mahanti
Department of Physics and Astronomy, Michigan State University, East Lansing, Michigan 48824, USA
(Received 26 September 2009; revised manuscript received 14 March 2010; published 14 April 2010)

Recent revival of interest in high-temperature (T) thermoelectrics has made it necessary to understand in detail the T dependence of different transport coefficients, and different processes contributing to this temperature dependence. Since PbTe is a well-studied prototypical high-temperature thermoelectric, we have carried out theoretical studies to analyze how different physical sources contribute to electronic transport coefficients in this system over a wide T and concentration (n) range; 300 K$<T<$900 K and $1<n/n_o<10$, where $n_o=10^{19}$ cm^{-3}, extending earlier works on this problem. We have used Boltzmann equation within energy-dependent relaxation time approximations. Although the T dependence of the electrical conductivity σ comes from several sources (band structure parameters, chemical potential μ, relaxation time τ), we find that the T dependence of τ dominates. We fit the T and the energy (ε) dependence of the total relaxation time τ_{tot} by a simple function $\tau \sim aT^{-p}/(b+c\varepsilon^r)$, where a, b, c, p, and r are T and ε independent parameters but depend on n. Using this function, we find that for concentration range of interest, changing r which governs the energy dependence of scattering does not appreciably affect the T dependence of σ. Electronic thermal conductivities both at constant current J and constant electric field E were calculated using this τ to reexamine the validity of Wiedemann-Franz (WF) law in PbTe, extending the earlier work of Bhandari and Rowe to higher temperatures. We find that using standard WF law to obtain the electronic contribution of the thermal conductivity (κ_{el}) usually overestimates this contribution by more than 0.5 WK^{-1} m^{-1}. Therefore the value of the lattice thermal conductivity obtained by subtracting this κ_{el} from the total thermal conductivity is underestimated roughly by the same amount.

DOI: 10.1103/PhysRevB.81.165203 PACS number(s): 72.10.Di, 71.20.Nr, 72.20.Pa

I. INTRODUCTION

Thermoelectric devices are generally made from heavily doped narrow band-gap semiconductors and are used both as generators and refrigeration devices without any moving parts or bulk fluids.[1] The efficiency of thermoelectric (TE) energy conversion depends on the transport coefficients of the constituent materials through the figure of merit (FOM) $ZT=\sigma S^2T/(\kappa_l+\kappa_{el,J})$, where σ is the electrical conductivity and S is the thermopower (Seebeck coefficient). The quantity in the denominator is the total thermal conductivity; it is given by the sum of contributions from the electronic carriers at constant electrical current J ($\kappa_{el,J}$) and the lattice contribution κ_l. Z has units of inverse temperature, so it is generally quoted as ZT, with T the average operating temperature of the TE device.[2] From the definition of the ZT it is clear that to increase ZT we have to decrease the thermal conductivity of the material and/or increase the thermopower and the electrical conductivity. Among the four quantities involved in ZT, three (σ, S, and $\kappa_{el,J}$) are mainly related to the electronic structure of the material and the fourth one (κ_l) primarily depends on the lattice. One possible way to improve the FOM is to reduce κ_l without significantly altering the electronic properties of the materials, referred to as electron crystal phonon glass concept.[3] This approach has been explored extensively in the past[4,5] through the enhancement of phonon scattering. The other way to increase FOM is to increase the power factor σS^2 by varying the doping concentration and manipulating the electronic structure in the neighborhood of the chemical potential.[6,7] In this paper we focus on the second approach taking PbTe as an example. Before one can increase the power factor in this system by manipulating its electronic structure one must understand in detail how the electronic structure and different scattering mechanisms affect σ and S in PbTe itself. Also we look at electronic contributions to the thermal conductivity $\kappa_{el,J}$ to see under what conditions it becomes small.

PbTe is a narrow band-gap semiconductor and is well known for its excellent thermoelectric properties. It is used for power generation in the temperature range 400–800 K.[8] Iodine and PbI_2 are the dopants used to optimize the carrier concentration in n-type PbTe.[1] However the lattice thermal conductivity of PbTe with these dopants is usually too high and limits its application (ZT is ~0.9 at 650K).[1] Therefore many methods have been used to reduce its κ_l, such as hot pressing and spark plasma sintering (SPS).[9] The value of κ_l for samples prepared by hot pressing is about 2 WK^{-1} m^{-1}, which is still higher than the ideal value of 1 WK^{-1} m^{-1} needed for good thermoelectric materials.[10] Although there are many successful examples of reducing the thermal conductivity in $Pb_{1-x}Sn_xTe$ $(Bi_{1-x}Sb_x)_2Te_3$ solid solutions,[10] recently, novel bulk quaternary systems $AgPb_mSbTe_{m+2}$ (LAST-m) with special m values,[11] PbSeTe/PbTe quantum dot (QD) superlattices,[12] have been found to give a large $ZT \sim 1.5-2$ in the temperature range (400–800 K).

A different approach to increase ZT by increasing the power factor has been suggested recently by Heremans and collaborators[13] and by Kanatzidis and collaborators.[14] The idea is to alter the energy dependence of the carrier scattering rate by inserting metallic nanoparticles such as Pb or Sb inside bulk PbTe. The precise effect of these nanoparticles (~30–50 nm size) on electronic and phononic transport properties is not known. One of the motivation of the present work is to see whether changing the energy dependence of the effective scattering time (rather than individual scattering

processes) affects the T dependence of electronic conductivity. From the theoretical side, several calculations of the transport coefficients (mainly σ and S) of PbTe and related systems have been reported over the years.[6,13,15–17] These calculations have been performed using Boltzmann transport equation within the energy-dependent relaxation time and the nonparabolic Kane model for energy dispersion $\varepsilon_{\vec{k}}$ vs $\vec{k}$. The energy and temperature dependence of different scattering mechanisms were incorporated in these calculations. Depending on the temperature range, different scattering mechanisms (such as from impurities, acoustic and optical phonons) made dominant contribution to the relaxation time. At high temperatures when optical phonons dominate the scattering mechanism, it was found that both polar and deformation coupling with optical phonons played equally important role (see Zayachuk[18] and Freik *et al.*[19]). Earlier work by Bhandari and Rowe[16] focused on the electronic thermal conductivity $\kappa_{el,J}$ (Ref. 16); they pointed out that the inclusion of nonparabolicity in energy dispersion had a pronounced effect on the electronic contribution to the thermal conductivity and neglecting it would overestimate $\kappa_{el,J}$. Also they pointed out that acoustic phonon scattering was the dominant carrier scattering mechanism in PbTe at room temperature (RT). In a later work, Bilc *et al.*[15] focused on the power factor at high temperatures, and showed that the strength of the deformation coupling constant had to be reduced by ~30% from its earlier value (used in fitting to the RT data) to get a better quantitative fit to the high T transport data.

All these earlier work did not explore the relationship between the energy and temperature dependence of the effective relaxation rate and the T dependence of σ, $\kappa_{el,J}$ and $\kappa_{el,E}$. Also a careful analysis of the difference between these two types of electronic thermal conductivities (constant E vs constant J) and its impact on the Wiedemann-Franz (WF) law (see below) was not made. In this paper we address these issues by focusing on (i) a careful analysis of the energy and T dependence of τ to develop a simple analytic form, (ii) understanding the relation between the energy dependence of τ and the T dependence of σ, S and the power factor (σS^2), and (iii) finding out the difference between electronic thermal conductivity at constant E and at constant J and reexamine the validity of WF law $\kappa_{el} \equiv \kappa_{el,E} = L_0 \sigma T$, where the Lorentz number $L_0 = 2.45 \times 10^{-8}\ W\Omega/K$.

Although the validity of using WF law to estimate electronic thermal conductivity at high temperatures has been questioned in the literature,[16] it is still widely used to estimate the lattice thermal conductivity from the total experimental thermal conductivity. The lattice thermal conductivities estimated this way are turning out to be very small, well below the so called alloy limit. This reduction has been attributed to the enhanced phonon scattering from the nanostructures present in the samples. Thus to have a more definite estimate of the phonon contribution to the thermal conductivity one must critically examine the use of WF law. Furthermore the difference between constant J and constant E electronic thermal conductivities in PbTe has not been addressed properly although the fact that the experimentally measured electronic thermal conductivity κ_{el} appearing in the expression for ZT is $\kappa_{el} = L\sigma T$, and the modified Lorentz number L is different from L_0 is well known.[16]

The arrangement of this paper is as follows. In Sec. II, we discuss the transport coefficients using the Boltzmann equation and define the transport functions. In Sec. III, we briefly review the nonparabolic Kane model for the energy band dispersion. In Sec. IV, we introduce transport coefficients in the Kane Model. In Sec. V, we describe the different scattering mechanisms contributing the total relaxation time in PbTe. In Sec VI, we discuss the total thermal conductivity and the different types of electronic contributions. In Sec VII, we present our results and discussions and, finally, we give a brief summary in Sec. VIII. We give the main equations in the text. The detailed expressions for different contributions to the relaxation time obtained using the Kane model are given in Appendixes A and B.

II. TRANSPORT COEFFICIENTS USING THE BOLTZMANN EQUATION

A standard method to deal with charge and energy transport is to use the Boltzmann transport equation.[20] In the relaxation time approximation, the different transport coefficient tensors, $\overleftrightarrow{\sigma}$ electrical conductivity, $\overleftrightarrow{S}$ thermoelectric coefficient or thermopower, and $\overleftrightarrow{\kappa}_{el,E}$ electronic thermal conductivity at zero electric field $\vec{E}$ rather than at zero current $\vec{J}$ are given by[20]

$$\overleftrightarrow{\sigma} = \frac{e^2}{V}\sum_{\vec{k}} \left(-\frac{\partial f_{\vec{k}}}{\partial \varepsilon_{\vec{k}}}\right) \tau_{\vec{k}} \vec{v}_{\vec{k}} \vec{v}_{\vec{k}}, \tag{1}$$

$$\overleftrightarrow{S} = (\overleftrightarrow{\sigma})^{-1} \overleftrightarrow{A}, \tag{2}$$

$$\overleftrightarrow{\kappa}_{el,E} = \frac{1}{VT}\sum_{\vec{k}} \left(-\frac{\partial f_{\vec{k}}}{\partial \varepsilon_{\vec{k}}}\right) (\varepsilon_{\vec{k}} - \mu)^2 \tau_{\vec{k}} \vec{v}_{\vec{k}} \vec{v}_{\vec{k}}, \tag{3}$$

where $\overleftrightarrow{A}$ tensor is given by

$$\overleftrightarrow{A} = \frac{e}{VT}\sum_{\vec{k}} \left(-\frac{\partial f_{\vec{k}}}{\partial \varepsilon_{\vec{k}}}\right) (\varepsilon_{\vec{k}} - \mu) \tau_{\vec{k}} \vec{v}_{\vec{k}} \vec{v}_{\vec{k}}. \tag{4}$$

In Eqs. (1), (3), and (4), e is electronic charge, V is the volume in real space, $\tau_{\vec{k}}$ is the crystal momentum $\vec{k}$ dependent relaxation time, $\vec{v}_{\vec{k}}$ is the velocity of charge carriers, and $f_{\vec{k}}$ is the equilibrium Fermi distribution function at temperature T and μ is the chemical potential.

III. NONPARABOLIC KANE MODEL FOR ENERGY DISPERSION

The band structure of PbTe is very well studied. Since the transport properties of interest depend on the band structure near the conduction band minima and valence band maxima there have been several attempts to describe the band structure using effective mass models. The most widely used effective mass model is that of Kane, called the Kane model.[21] In this section we will briefly review the Kane model valid near the band extrema which occur at the L point of the

Brillouin zone (BZ). In narrow band-gap semiconductors (i.e., lead chalcogenides) the energy region of interest of an electron as measured from the band edge is comparable to the band gap E_g. Because of this, the dependence of the energy on crystal momentum is nonparabolic and the effective masses are functions of the energy. The nonparabolic Kane model was introduced to describe the deviations from the quadratic dependence of energy on the crystal momentum. In this model, the longitudinal effective mass m_l and the transverse effective mass m_t depend only on the interaction between the lowest conduction band and the highest valence band and the contributions of other bands are assumed to be small. Here longitudinal and transverse are defined parallel and perpendicular to the vector joining the center of the BZ to the L point. For a simple anisotropic parabolic model the energy dispersion can be expressed as

$$\varepsilon_{\vec{k}} = \frac{\hbar^2}{2}\left(\frac{2k_t^2}{m_t} + \frac{k_l^2}{m_l}\right), \tag{5}$$

where $\varepsilon_{\vec{k}}$ is the energy, and k_l and k_t are the magnitudes of the longitudinal and transverse components of $\vec{k}$, measured from the band extrema. In the Kane model the energy dispersion is given by[21]

$$\varepsilon_{\vec{k}}\left(1 + \frac{\varepsilon_{\vec{k}}}{E_g}\right) = \frac{\hbar^2}{2}\left(\frac{2k_t^2}{m_t} + \frac{k_l^2}{m_l}\right), \tag{6}$$

where E_g is the band gap. Also in this model the effective masses and the mass anisotropy coefficients of electrons and holes are equal. The constant energy surfaces are ellipsoids, and m_l and m_t have the same energy dependence.

IV. TRANSPORT COEFFICIENTS IN THE KANE MODEL

In order to calculate the transport coefficients using the Kane model we have to compute different quantities appearing in Eqs. (1)–(4), which include the carrier velocity $\vec{v}_{\vec{k}}$ and the relaxation time $\tau_{\vec{k}}$. The expressions for the transport coefficient have been obtained by Ravich *et al.*[22,23] and Bilc *et al.*[15] The basic expressions are given below and the detailed equations are given in Appendixes A and B.[18,19,22,23]

PbTe is cubic and therefore the components $\sigma_{\mu\nu}$, $S_{\mu\nu}$, and $(\kappa_{el,E})_{\mu\nu}$ of the electrical conductivity and thermopower tensors can be expressed as

$$\sigma_{\mu\nu} = \delta_{\mu\nu}\sigma, \tag{7}$$

$$S_{\mu\nu} = \delta_{\mu\nu}S, \tag{8}$$

$$(\kappa_{el,E})_{\mu\nu} = \delta_{\mu\nu}\kappa_{el,E}, \tag{9}$$

where σ, S, and $\kappa_{el,E}$ are related to the trace of $\overleftrightarrow{\sigma}$, $\overleftrightarrow{S}$, and $\overleftrightarrow{\kappa}_{el,E}$ tensors and are given by: $\sigma = \frac{1}{3}\mathrm{Tr}\,\overleftrightarrow{\sigma}$; $S = \frac{1}{3}\mathrm{Tr}\,\overleftrightarrow{S}$; $\kappa_{el,E} = \frac{1}{3}\mathrm{Tr}\,\overleftrightarrow{\kappa}_{el,E}$. For the cubic system, Tr $\overleftrightarrow{\sigma}$, Tr $\overleftrightarrow{\sigma}$, and Tr $\overleftrightarrow{\kappa}_{el,E}$ are related to $\vec{v}_{\vec{k}}\vec{v}_{\vec{k}} = \vec{v}_{\vec{k}}^2$ terms. Using simple scaling transformations (see Appendix A) one can calculate the transport coefficients. The three transport coefficients σ, S, and $\kappa_{el,E}$ can be expressed in terms of a single transport function $\Sigma(\varepsilon)$, i.e.,

$$\sigma = e^2\int_0^\infty d\varepsilon\left(-\frac{\partial f}{\partial \varepsilon}\right)\Sigma(\varepsilon,T), \tag{10}$$

$$S = \frac{e}{T\sigma}\int_0^\infty d\varepsilon\left(-\frac{\partial f}{\partial \varepsilon}\right)\Sigma(\varepsilon,T)(\varepsilon-\mu), \tag{11}$$

$$\kappa_{el,E} = \frac{1}{T}\int_0^\infty d\varepsilon\left(-\frac{\partial f}{\partial \varepsilon}\right)\Sigma(\varepsilon,T)(\varepsilon-\mu)^2, \tag{12}$$

where $\Sigma(\varepsilon,T) = \frac{1}{V}\Sigma_{\vec{k}}\delta(\varepsilon_{\vec{k}}-\varepsilon)\tau_{\vec{k}}\vec{v}_{\vec{k}}\vec{v}_{\vec{k}}$ is given by

$$\Sigma(\varepsilon,T) = \frac{2}{3}\gamma\frac{(2m_d')^{1/2}}{\pi^2\hbar^3}\left[\varepsilon\left(1+\frac{\varepsilon}{E_g}\right)^{3/2}\left(1+\frac{2\varepsilon}{E_g}\right)^{-1}\right]\tau(\varepsilon,T). \tag{13}$$

The parameter γ is the degeneracy of the conduction and valence bands m_d' is an average effective mass parameter defined in Appendix A. Some of the T dependence of the transport function comes indirectly from the T dependence of these parameters. The relaxation time $\tau(\varepsilon,T)$ depends on energy and temperature; the T dependence comes indirectly from the T dependence of the electronic structure and μ.

The concentration of carriers n for the Kane model is given by

$$n = \frac{2^{1/2}}{\pi^2\hbar^3}\gamma m_d'^{3/2}\int_o^\infty \frac{\left[\varepsilon\left(1+\frac{\varepsilon}{E_g}\right)\right]^{1/2}\left(1+\frac{2\varepsilon}{E_g}\right)d\varepsilon}{\exp\left(\frac{\varepsilon-\mu}{k_BT}\right)+1} \tag{14}$$

The expression $\gamma m_d'^{3/2}$ can be expressed in terms of a single effective mass parameter $m_d^{3/2} = \gamma m_d'^{3/2}$, where m_d is called density of state effective mass because it takes into account the degeneracy of the conduction (valence) band. The derivation of the relations between scaling mass parameter (m_d'), the density of state effective mass m_d and longitudinal and transverse effective masses (m_l, m_t) are discussed in Appendix A. The scaling mass parameter $m_d' = (m_l m_t^2)^{1/3}$ and $m_d = \gamma^{2/3}m_d' = \gamma^{2/3}(m_l m_t^2)^{1/3}$.

V. RELAXATION TIMES IN THE KANE MODEL

Different scattering mechanisms of charge carriers in lead chalcogenides have been extensively discussed in many papers.[17,19,22,23] The total scattering rate $1/\tau_{tot}$ is expressed as a summation of different contributions: acoustic phonons (a), optical phonons with deformation coupling (o), optical phonons with polar coupling (po), vacancies (v), and coulomb scattering from charged impurities (C),

$$\frac{1}{\tau_{tot}} = \frac{1}{\tau_a} + \frac{1}{\tau_o} + \frac{1}{\tau_{po}} + \frac{1}{\tau_v} + \frac{1}{\tau_C}. \tag{15}$$

The expressions for different contributions to the relaxation time within the Kane model were first worked out by Ravich and collaborators and later extended by Zayachuck and Freik *et al.*[19,22,23] They are available in the literature. We give the final expressions for different scattering mechanisms in Ap-

TABLE I. Parameters used to calculate the relaxation times for PbTe (Refs. 15 and 18).

Parameter	Unit of measurement	Value
m_l/m		0.24
ϵ_0		400
ϵ_∞		32.6
C_l	N/m^2	0.71×10^{11}
ω_0	eV	0.0136
a	Å	6.461
ρ	g/cm^3	8.24
Z		0.14
E_{ac}	eV	15
N_v	cm^{-3}	2.5×10^{19}
E_{oc}	eV	15
U_{vc}	Erg cm^3	3×10^{-34}
K_a,K_o,K_v for n-type		1.0
K_a,K_o,K_v for p-type		1.5

pendix B. Here we discuss the fundamental parameters involved in the calculations of different relaxation rates and analyze their relative significance for the PbTe system.

In general, it is found that the dominant scattering mechanisms contributing to τ_{tot} are from the point defects and thermal phonons. At low temperatures (liquid helium), charge carriers are scattered mostly by charged vacancies. At low densities $n\leq5\times10^{18}$ cm^{-3}, scattering by Coulomb potential of the vacancies dominates, whereas for high carrier densities $n\geq10^{19}$ cm^{-3}, the Coulomb potential gets screened out and scattering by the short range potential of vacancies dominates. As the temperature increases, the relative importance of the charged vacancies decreases and scattering by thermal phonons increases. For temperatures above 300 K, scattering by acoustic phonons and optical phonons (both polar and deformation potential coupling) contribute to τ_{tot}.

The parameters we have used to calculate the relaxation time were taken from Ref. 18 where the transport data were fitted in the temperature range 300 $K<T<900$ K. They are given in Table I. Experimentally, one finds that the energy gap E_g and the density of states effective mass m_d are temperature dependent.[24] This comes from strong electron-phonon coupling. Following the work of Bilc *et al.*,[15] we have incorporated the T-dependent E_g and m_d using the experimental data. It turns out that the temperature dependence of m_d is very important to get a good agreement between theoretical and measured values of the transport coefficients σ and S.[15] Experimentally, it is found that E_g increases linearly with temperature for $T\leq400$ K and above 400 K, it remains constant. The temperature dependence of the band gap E_g (Ref. 24) can be approximately given as

$$E_g = 0.19 + (0.42\times10^{-3})T \quad \text{for} \quad T\leq400\ \text{K}, \tag{16}$$

$$E_g = 0.358 \quad \text{for} \quad T>400\ \text{K} \tag{17}$$

The temperature dependence of the density of states effective mass m_d comes primarily from the temperature dependence of the transverse effective mass m_t and this is taken from experiment,[25,26]

$$\frac{m_t}{m} = 0.02459 + (8.659341\times10^{-5})T, \tag{18}$$

where m is the bare electron mass. In Eqs. (16) and (17), the energies are in eV and the coefficient of T is in eV/K. Similarly the coefficient of T in Eq. (18) is in the units of 1/K.

Before discussing the detail results of our present study we make a few brief comments on the work of Bhandari and Rowe[16] and Bilc *et al.*[15] Bhandari *et al.* considered the deformation potential of acoustic phonon as the dominant scattering mechanism (τ_a) at room temperature although they claimed that scattering by polar optical modes might not be insignificant. On the other hand, Bilc *et al.*[15] focused on the high temperature transport coefficients (but considered only σ and S) and included all the scattering contributions. The latter authors did not however explicitly explore the energy and T dependence of the relaxation time and how they contributed to the T dependence of σ and S. In this paper we address this specific question.

In Table II, we give the contribution of each scattering mechanism to the scattering rate for different temperatures ($T\geq300$ K) and different values of the carrier energy ε. Scattering by acoustic phonons and optical phonons (both polar and deformation potential coupling) make significant contributions at temperatures above 300 K. The contribution of the vacancies both due to their short range deformation potential (τ_v) and their long range Coulomb potential (τ_C) at are small and insignificant in this temperature range. At low energies ($\varepsilon\ll0.10$ eV), the polar scattering by optical phonons (τ_{po}) dominates, whereas in the energy range ($0.1\leq\varepsilon\leq0.30$) eV scattering by acoustic phonons and optical phonons (both polar and deformation potential coupling) are comparable. For higher energies ($\varepsilon>0.30$ eV), the acoustic phonon scattering is dominant. At constant temperature, the contributions from τ_a and τ_o increase with ε whereas the contribution from τ_{po} decreases with ε.

In Fig. 1, we plot the inverse relaxation time associated with the three dominant scattering mechanisms (τ_a, τ_o, and τ_{po}) as a function of carrier energy ε, for different T (300, 600, and 900 K) for carrier density $n=5\times10^{19}$ cm^{-3}. The chemical potential μ was calculated for each T (T dependence of μ will be discussed latter in Sec. VI). Also, we have drawn $(-\partial f_0/\partial\varepsilon)$, in order to see the energy range ε that contribute to the transport coefficients and hence check the scattering mechanisms that contribute in this range. We can see from Fig. 1 that, in the range ($0<\varepsilon<0.3$ eV), it is not appropriate to ignore the deformation potential (τ_0^{-1}) and polar (τ_{po}^{-1}) scattering by optical phonons to get a correct understanding of the transport coefficients and subsequent comparison with experiment (see Ref. 15). At room temperature $T=300$ K where $\mu=0.146$ eV, we find that τ_a and τ_{po} are comparable and τ_o is not insignificant. Increasing temperature reduces μ and therefore shifts the $(-\partial f_0/\partial\varepsilon)$ peak toward a lower energy, as shown from Figs. 1(b) and 1(c). This increases the contribution of the polar scattering by optical phonons to the net scattering rate.

TABLE II. Inverse of the relaxation time of different scattering mechanisms in PbTe for different temperatures T and different carrier energies ε.

	$1/\tau_a$ (10^{11} sec^{-1})	$1/\tau_o$ (10^{11} sec^{-1})	$1/\tau_{po}$ (10^{11} sec^{-1})	$1/\tau_v$ (10^{11} sec^{-1})	$1/\tau_c$ (10^{11} sec^{-1})	ε (eV)
300 K	14.90	7.12	75.70	0.996	0.25	
600 K	45.10	21.50	198.00	1.51	0.22	0.02
900 K	129.00	61.70	315.00	2.88	0.09	
300 K	36.60	17.50	56.60	2.44	0.02	
600 K	109.00	51.80	136.00	3.62	0.02	0.10
900 K	246.00	118.00	221.00	5.48	0.02	
300 K	63.60	30.30	48.60	4.24	0.01	
600 K	183.00	87.20	112.00	6.10	0.01	0.20
900 K	400.00	191.00	186.00	8.91	0.01	
300 K	97.10	46.30	45.70	6.48	0.004	
600 K	272.00	130.00	103.00	9.08	0.004	0.30
900 K	587.00	280.00	172.00	13.10	0.004	

VI. THERMAL CONDUCTIVITY

The total thermal conductivity κ_{tot} is usually defined and measured at constant current (J) and is a sum of the lattice contribution κ_l and the electronic part $\kappa_{el,J}$. It is given by

$$\kappa_{tot} = \kappa_l + \kappa_{el,J}, \tag{19}$$

$$= \kappa_l + \kappa_{el,E} - T\sigma S^2, \tag{20}$$

where $\kappa_{el,E}$ is the electronic thermal conductivity at constant electric field (E). This κ_{tot} appears in the definition of ZT.[2] In the literature some times one uses κ_{el} without explicitly telling whether it is a constant J or constant E. For degenerate metals where S is very small or for semiconductors with very small carrier concentration and hence σ, the quantity $T\sigma S^2$ is very small and $\kappa_{el,J} \approx \kappa_{el,E} \approx \kappa_{el}$. But for good thermoelectrics $T\sigma S^2$ is quite large and the two thermal conductivities differ. In fact, for a thermally stable electronic system both $\kappa_{el,E}, \kappa_{el,J} \geq 0$. The dimensionless figure of merit for a thermoelectric is given by

$$ZT = \frac{T\sigma S^2}{\kappa_l + \kappa_{el,E} - T\sigma S^2}, \tag{21}$$

and can be optimized by manipulating $\kappa_{el,E}$. Sofo and Mahan[26] found that for a given lattice thermal conductivity κ_l, the best thermoelectric is when $\kappa_{el,E} = T\sigma S^2$, which is equivalent to $\kappa_{el,J} = 0$. If we look at Eqs. (10)–(12) this equality occurs when $\Sigma(\varepsilon, T) = A\delta(\varepsilon - \varepsilon_0)$, i.e., the energy and charge transport take place in a single energy channel, $\varepsilon = \varepsilon_0$, i.e., perfect energy filtering. Even in this case one has to adjust the chemical potential such that $|\mu - \varepsilon_0| \approx 2.5 k_B T$ to maximize ZT. In this case $ZT \to \infty$ when the lattice thermal conductivity is ignored ($\kappa_l = 0$). In a recent work Humphrey and Linke[27] explored a similar energy filtering idea, but for an inhomogeneous system. They have shown that in the presence of a temperature gradient, if one can construct a graded thermoelectric such that the quantity $(\varepsilon(\vec{r}) - \mu)/k_B T(\vec{r})$ remains constant throughout the sample, then the energy and charge transport is adiabatic, which gives rise to perfect Carnot efficiency. This correspond to $ZT = \infty$, when $\kappa_l = 0$. In this limit the thermoelectric efficiency given by[2]

$$\eta = \frac{T_{hot} - T_{cold}}{T_{hot}} \left(\frac{\sqrt{1+ZT} - 1}{\sqrt{1+ZT} + \frac{T_{cold}}{T_{hot}}} \right) \to (T_{hot} - T_{cold})/T_{hot}$$

$$= \eta_{carnot}. \tag{22}$$

VII. RESULTS AND DISCUSSIONS

As mentioned in Sec. V, we have taken into account the temperature dependence of the energy gap E_g and the density of states effective mass m_d, which are given in Eqs. (16)–(18). In PbTe, the gap occurs at the L point in the fcc BZ and the degeneracy parameter $\gamma = 4$. At high concentrations, $n \sim 10^{19}$ cm^{-3}, which are required for a good thermoelectric, the n- or p-type PbTe can be described using a single (either conduction or valence) band model since for these concentrations, contributions to transport come primarily from one type of carrier. (Note that for p-type transport all transport equations have to be interpreted in terms of hole occupation function.) Here we give the results for the n-type PbTe. Figure 2 shows the temperature dependence of the chemical potential μ for concentrations $n = 5 \times 10^{19}$ cm^{-3} and $n = 5 \times 10^{20}$ cm^{-3}. The change in μ over the temperature range of 300–900 K is quite significant. This plays an important role in the observed T dependence of σ, S and $\kappa_{el,E}$ over this temperature range. In Fig. 3 we compare our theoretical results for σ and S with experiment, taken from Ref. 28. The parameters used to calculate τ_{tot} were taken from Bilc *et al.*'s. work.[15] Our theoretical results for $\kappa_{el,E}$ and $\kappa_{el,J}$ will be discussed below (Sec. VII B).

A. Energy and temperature dependence of the relaxation time

The temperature and energy dependence of the total relaxation time τ_{tot} is shown in Fig. 4. The τ_{tot} decreases with

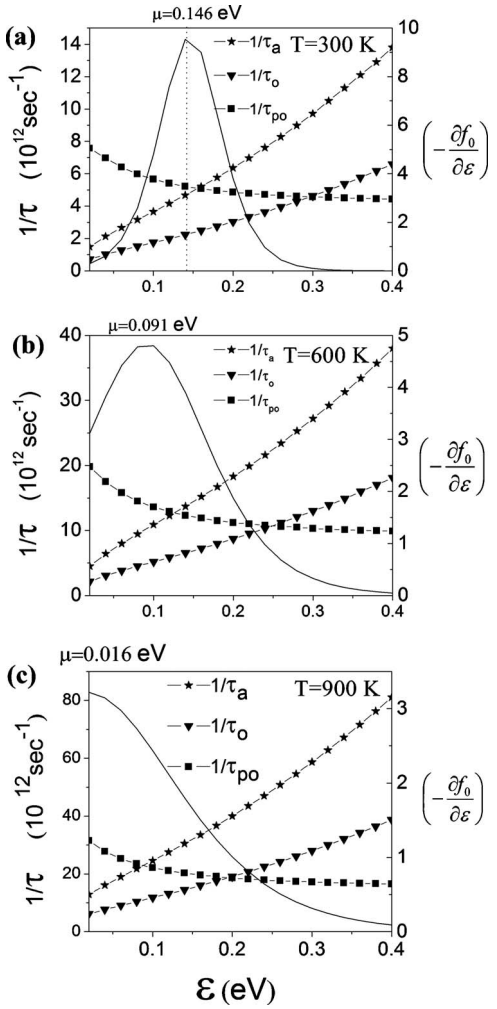

FIG. 1. Energy dependence of the inverse of the relaxation time of the three dominant scattering mechanisms (τ_a, τ_o, and τ_{po}) in PbTe for electron carrier density $n=5\times10^{19}$ cm^{-3} at different temperatures (a) 300 K, (b) 600 K, and (c) 900 K. The smooth curves gives the $(-\partial f_0/\partial\varepsilon)$ indicating the energy region contributing to the transport at different temperatures.

increasing ε for a given T and decreases with increasing T for a given ε. We have scaled τ_{tot} for different temperatures in order to see how the scaled τ_{tot} depends on ε. Figure 5

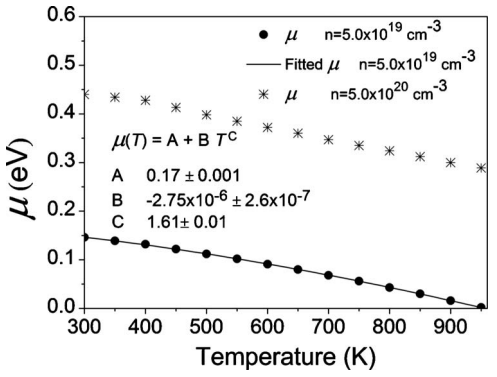

FIG. 2. Temperature dependence of the chemical potential μ for n-type PbTe at different concentrations $n=5\times10^{19}$ cm^{-3} and $n=5\times10^{20}$ cm^{-3}.

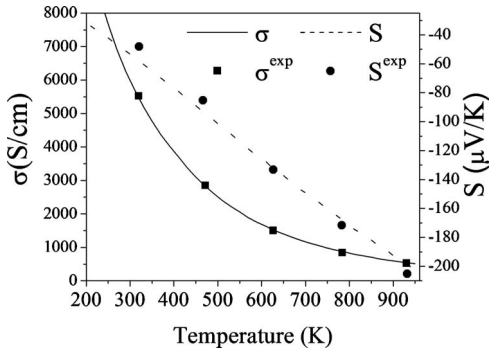

FIG. 3. Temperature dependence of the electrical conductivity σ and thermopower S for n-type PbTe at concentration $n=5\times10^{19}$ cm^{-3}. The experimental values are shown as solid points.

shows that for different T, the energy dependence of τ_{tot} is almost the same; therefore we fit $\tau_{tot}(T=300\ \mathrm{K},\varepsilon)$ to find the energy dependence of τ_{tot} (see Fig. 6). After that it is straight forward to find the T dependent of the parameter $F(T)$ that appears in the fitted analytic expression for τ_{tot} (see below and Fig. 7). The total relaxation time of PbTe can be approximated extremely well by a scaling function

$$\tau_{tot} = \frac{aT^{-p}}{(b + c\varepsilon^r)}, \tag{23}$$

where a, b, c, p, and r are T and ε independent parameters but depend only on the carrier concentration n. We have used this expression to check the calculated electrical conductivity σ and the thermopower S, (see Figs. 8 and 9). The scaling expression for τ_{tot} gives excellent agreement (within 5%) with the values of σ and S calculated directly by considering contributions from different scattering mechanisms.

To check how sensitive the electrical conductivity σ is to the energy dependence of τ_{tot}, we plot σ for different values of the parameter r [see Eq. (23)] in Fig. 10. The absolute values of σ change with r. As r increases from 0 scattering in the energy range of interest (0.0–0.3 eV as discussed in Sec. V) gets suppressed leading to an increase in σ for all T. However, after scaling the values of σ for different temperatures, we notice that the T dependence $\sigma\sim T^{-2.2}$ is not sen-

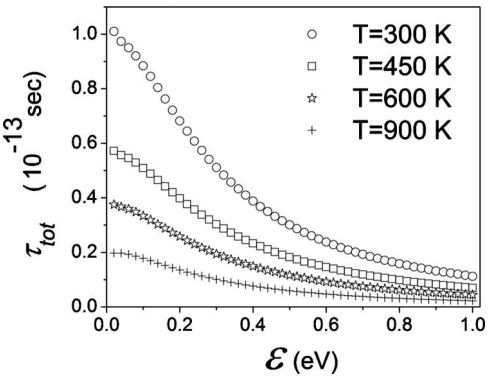

FIG. 4. Energy dependence of the total relaxation time τ_{tot}, calculated from Eq. 5.80, for n-type PbTe at concentration $n=5\times10^{19}$ cm^{-3} for different temperatures.

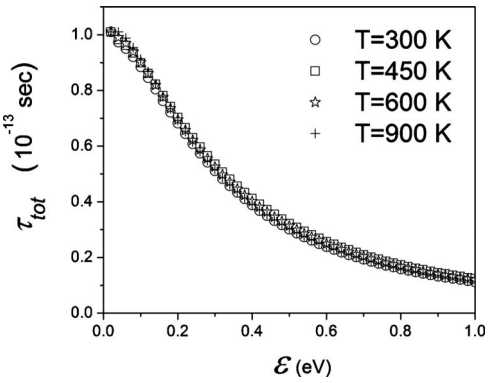

FIG. 5. Energy dependence of the scaled (to 300 K) total relaxation time τ_{tot} at different temperatures.

sitive to the energy dependence of τ_{tot} in the temperature and concentration range of interest. In order to understand both the temperature dependence of σ and why it is so weekly dependent on the parameter r, we look in detail the different physical quantities that give rise to the observed T dependence of σ. The scaling form [Eq. (23)] gives $\tau_{tot} \sim T^{-p}$, $p=1.4$. This power-law dependence comes from two sources, T^{-1} dependence from the phonon occupation number at high T ($k_B T \gg \hbar\omega$), $\tau^{-1} \sim (k_B T)/(\hbar\omega)$ and a $T^{-0.4}$ dependence from the temperature dependence of the density of states through the parameter m_{d0} (see Sec. V for different phonon induced relaxation rates). The question is where the additional $T^{-0.8}$ dependence of σ comes from. In order to answer this, we made a simple calculation. We assumed τ_{tot} to be constant and then calculated the T dependence of σ coming from other sources. We find that $\sigma \sim T^{-0.8}$, the T dependence of the chemical potential μ playing a crucial role in this T dependence. In this respect, PbTe at the doping levels of thermoelectric interest, differs qualitatively from both highly degenerate limit and the nondegenerate limit,[1] and is somewhere in between.

B. Electronic thermal conductivity and the validity of Wiedemann-Franz law

We will now use the full T and ε dependence of the effective relaxation time [using our scaled form, Eq. (23)], T dependence of chemical potential and other parameters to

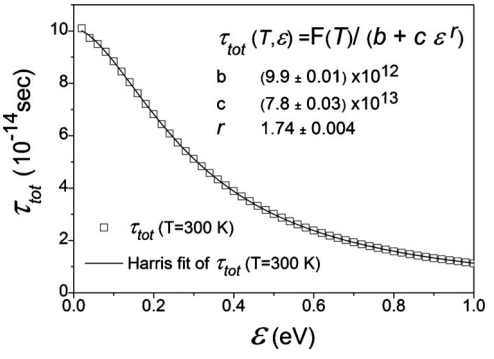

FIG. 6. Energy dependence of the total relaxation time τ_{tot} for $T=300$ K.

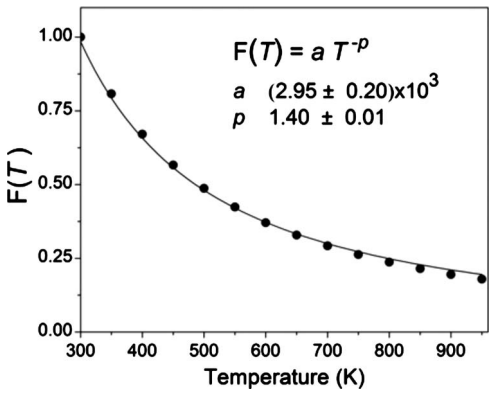

FIG. 7. Temperature dependence of the total relaxation time τ_{tot} at $\varepsilon=0.1$ eV.

look at the electronic thermal conductivity. This is a generalization of the earlier work by Bhandari and Rowe[16] who looked at this problem but only with acoustic phonon scattering. They found that the acoustic phonon scattering was the dominant scattering mechanism in PbTe at high temperature. Our calculations for τ_{tot}, as we discussed earlier in Sec. V, show that it is not appropriate to ignore the deformation potential τ_o and polar τ_{po} scattering by optical phonons if one wants to have a proper understanding of the transport coefficients at temperatures of interest. (Our results for the electronic thermal conductivity agrees perfectly with their results if we only consider the acoustic phonon scattering.) In Fig. 11 we give the T dependence of $\kappa_{el,E}$ and $\kappa_{el,J}$. Both decrease with T, but the difference increases with T. One question is how close PbTe is to a perfect thermoelectric $ZT=\infty$ when $\kappa_l=0$ [see Eq. (22)]. In this limit, $ZT=(\sigma S^2 T)/\kappa_{el,J} = (\kappa_{el,E}/\kappa_{el,J}) - 1$. We plot this quantity in Fig. 12, it goes from ~0.1 at 300 K (metallic limit) to ~3 at 900 K. PbTe does approach a perfect thermoelectric at high temperatures but is far from it.

Next we address the validity of Wiedemann-Franz (WF) law. The first question is whether $\kappa_{el,E}=L_0\sigma T$ or $\kappa_{el,J}=L_0\sigma T$ where the Lorentz number $L_0=2.45\times10^{-8}$ $W\Omega/K^2$. For a metal or a highly degenerate semiconductor it is the first equation that is correct.[2,20] One can use the calculated σ (Fig. 8) and this equation to estimate $\kappa_{el,E}$. However there is

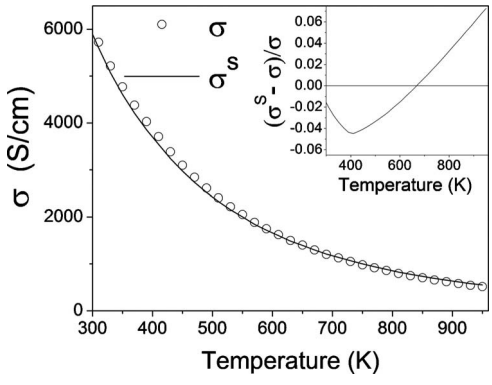

FIG. 8. A comparison between the electrical conductivity σ using the scattering mechanisms of the relaxation time with the scaled formula.

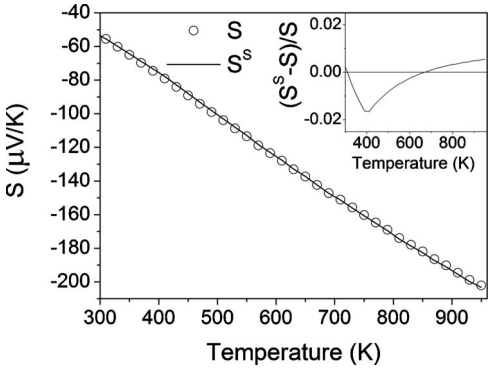

FIG. 9. A comparison between the thermopower S using the scattering mechanisms of the relaxation time with the scaled formula.

a fundamental problem. If we use this $\kappa_{el,E}$ and then estimate $\kappa_{el,J}$ using the calculated values of σ and S (the plot $L_0\sigma T - S^2\sigma T$ in Fig. 11), we find that for $T > 700$ K, $\kappa_{el,J} < 0$. But since $\kappa_{el,J}$ is a response function it must be positive definite. So we cannot use the equation $\kappa_{el,E} = L_0\sigma T$ to estimate $\kappa_{el,E}$ from experimental σ and then calculate $\kappa_{el,J}$ using the experimental value of σ and S.

The next thing we can do is to use the second equation, $\kappa_{el,J} = L_0\sigma T$. This appears to be more reasonable and is closer to the values of properly calculated $\kappa_{el,J}$. This is what is usually done in the estimation of electronic contribution to the total thermal conductivity κ_{tot} using experimental values of σ and S. As we can see in Fig. 11, the use of WF law overestimates the electronic contribution $\kappa_{el} \equiv \kappa_{el,J}$ and therefore underestimates the lattice contribution. The proper lattice contribution should be actually higher (by more than 0.5 W K^{-1} m^{-1}).

In order to find the temperature dependence of electronic thermal conductivity at constant current ($\kappa_{el,J}$), one defines an effective Lorentz number as[29]

$$L = \frac{\kappa_{el,J}}{\sigma T}. \tag{24}$$

Figure 13 shows the effective Lorenz number vs temperature for different carrier concentrations. As we can see, the effective Lorenz number L approaches L_0 (metallic like electric thermal conductivity) with increasing concentration and decreasing temperature. As pointed out in Sec. V, for a perfect thermoelectric $\kappa_{el,J} = 0$, i.e., $L = 0$.

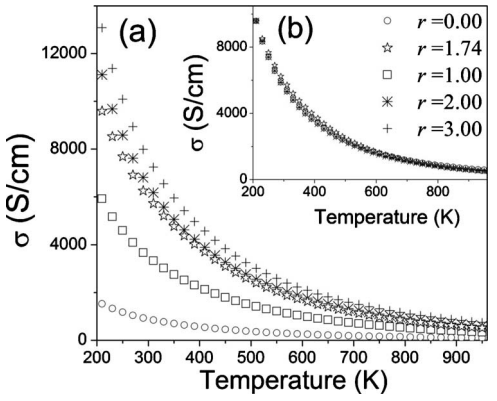

FIG. 10. (a) Temperature dependence of σ, using the scaling formula of the total relaxation time for different r parameter. (b) Temperature dependence of the scaled σ (to $r = 1.74$).

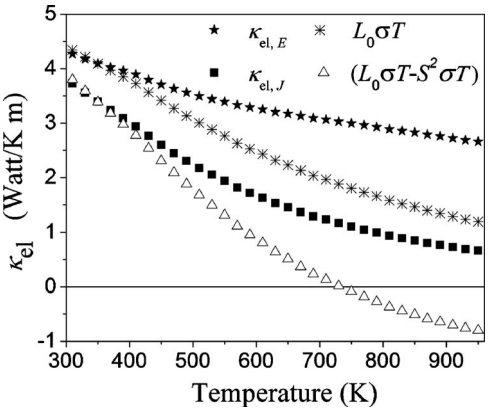

FIG. 11. Temperature dependence of the electronic thermal conductivity (κ_{el}) at constant electric field $E(\kappa_{el,E})$ and at constant current density $J(\kappa_{el,J})$ using Boltzmann transport equations. We also give their values using WF law.

VIII. SUMMARY

Transport calculations using the nonparabolic Kane model for energy dispersion in PbTe show that the deformation potential of acoustic phonons (τ_a), the deformation potential of optical phonons (τ_o), and the polar scattering by optical phonons (τ_{po}), are comparable and make significant contributions at temperatures above 300 K. Temperature and energy dependence of the total relaxation time τ_{tot} calculations show that the T dependence comes from two sources, one from the high-T limit of the phonon occupation number and the other from the density of states associated with the carriers. In the temperature range 300 K $< T <$ 900 K, the conductivity σ for n-type PbTe $\sim T^{-2.2}$. This T dependence comes from several sources such as band structure parameters, i.e., effective mass, chemical potential μ, and relaxation time τ_{tot}. The T dependence of τ_{tot} however dominates, the other important source being a strong T dependence of μ.

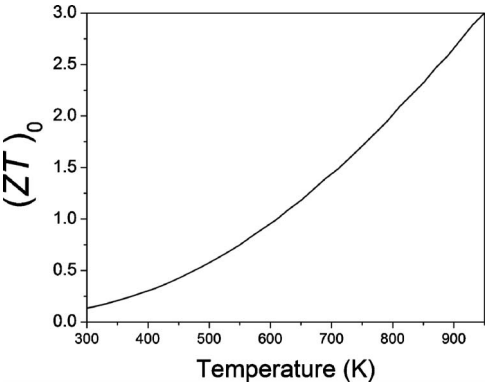

FIG. 12. Temperature dependence of ZT for n-type PbTe at concentration $n = 5 \times 10^{19}$ cm^{-3} assuming $\kappa_l = 0$.

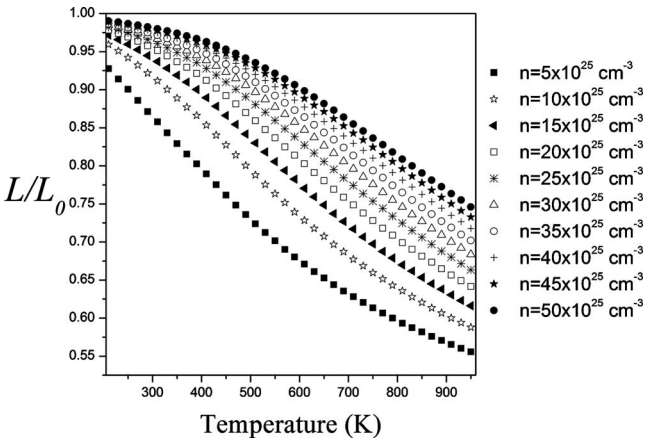

FIG. 13. Temperature dependence of the scaled effective Lorenz number (L/L_0) for n-type PbTe at different concentration n ($L_0 = 2.45 \times 10-8$ WΩ K^{-2}).

It turns out that energy dependence of $\tau_{tot}(T,\varepsilon)$ does not seem to control the T dependence of σ in this temperature range and for carrier concentration $n \sim (1-10) \times 10^{19}$ cm^{-3}. This should have implications on the current attempts to change the energy dependence of electron scattering to control the T dependence of σ. Careful electronic thermal conductivity calculations were done using the same model and parameters which were used to fit σ and S. Our calculations show that using WF law ($\kappa_{el,J}=L_0\sigma T$) to estimate this contribution of the thermal conductivity will overestimate the electronic contribution and hence underestimate the lattice contribution to the total thermal conductivity. This suggests that the very low values of lattice thermal conductivity found using WF law may not be quite right and should only provide a lower bound on the values of thermoelectric FOM, ZT, quoted in the literature.

ACKNOWLEDGMENTS

Financial support from the Office of Naval Research (Contract No. N00014-03-10789 MURI program) is gratefully acknowledged.

APPENDIX A

The Kane model for energy dispersion [Eq. (6) of the text] contains two types of effective masses and in order to simplify the calculations the following substitutions can be made:

$$k_t^2 = \frac{m_t}{m_d'} k_t'^2, \tag{A1}$$

$$k_l^2 = \frac{m_l}{m_d'} k_l'^2, \tag{A2}$$

where $m_d'=(m_l m_t^2)^{1/3}$ is a scaling mass parameter.[15]

Using the new variables k_l' and k_t', Eq. (6) can be rewritten as

$$\varepsilon_{k'}\left(1+\frac{\varepsilon_{k'}}{E_g}\right) = \frac{\hbar^2}{2m_d'}(2k_t'^2 + k_l'^2) \equiv \frac{\hbar^2}{2m_d'}k'^2. \tag{A3}$$

The carrier velocity is given by

$$\hbar\vec{v}_{\vec{k}'} = \frac{1}{\hbar}\frac{\partial\varepsilon_{\vec{k}'}}{\partial\vec{k}'} = \frac{\hbar}{m_d'}\frac{\vec{k}'}{1+\frac{2\varepsilon}{E_g}}. \tag{A4}$$

Using the above equation, the $v_{\vec{k}'}^2 = v_{\vec{k}'}.v_{\vec{k}'}$ term in the transport equations can be expressed as

$$v_{\vec{k}'}^2 = \frac{2}{m_d'}\frac{\varepsilon\left(1+\frac{\varepsilon}{E_g}\right)}{\left(1+\frac{2\varepsilon}{E_g}\right)^2}. \tag{A5}$$

Using Eq. (A3), the infinitesimal unit volume in reciprocal space $d^3\vec{k}'$ can be expressed as

$$d^3\vec{k}' = 4\pi k'^2 dk' = 4\pi\frac{2^{1/2}m_d'^{3/2}}{\hbar^3}\left[\varepsilon\left(1+\frac{\varepsilon}{E_g}\right)\right]^{1/2}\left(1+\frac{2\varepsilon}{E_g}\right)d\varepsilon. \tag{A6}$$

In terms of the new variable $\vec{k}'$, with changing the sums into integrals, and taking into account the spin degeneracy and band degeneracy γ, for the cubic system one obtains the Eqs. (13)–(15) of the text.

APPENDIX B

The expressions for the relaxation times from different mechanisms using the nonparabolic Kane model for PbTe are given below.

(i) Deformation potential of acoustic phonons (τ_a),

$$\tau_a = \frac{\tau_{0,a}(T)\left(\varepsilon+\frac{\varepsilon^2}{E_g}\right)^{-1/2}}{\left(1+2\frac{\varepsilon}{E_g}\right)[(1-A)^2-B]}, \tag{B1}$$

$$A = \frac{\frac{\varepsilon}{E_g}(1-K_a)}{\left(1+2\frac{\varepsilon}{E_g}\right)}, \tag{B2}$$

$$B = \frac{8\frac{\varepsilon}{E_g}\left(1+\frac{\varepsilon}{E_g}\right)K_a}{3\left(1+2\frac{\varepsilon}{E_g}\right)^2}, \tag{B3}$$

$$\tau_{0,a}(T) = \frac{2\pi\hbar^4 C_l}{E_{ac}^2 K_B T (2m_{d0})^{3/2}}, \tag{B4}$$

where E_{ac} is the acoustic deformation potential coupling constant for the conduction band, C_l is a combination of elastic

constants, K_a is the ratio of the acoustic deformation potential coupling constants for the valence and conduction bands $K_a=E_{av}/E_{ac}$ with the values $K_a=1$ for n-type PbTe and $K_a=1.5$ for p-type PbTe, and m_{d0} is the density of states effective mass for a single ellipsoid ($\gamma=1$).

(ii) Deformation potential of optical phonons (τ_o),

$$\tau_o = \frac{\tau_{0,o}(T)\left(\varepsilon+\frac{\varepsilon^2}{E_g}\right)^{-1/2}}{\left(1+2\frac{\varepsilon}{E_g}\right)[(1-A)^2-B]}, \tag{B5}$$

$$A = \frac{\frac{\varepsilon}{E_g}(1-K_o)}{\left(1+2\frac{\varepsilon}{E_g}\right)}, \tag{B6}$$

$$B = \frac{8\frac{\varepsilon}{E_g}\left(1+\frac{\varepsilon}{E_g}\right)K_o}{3\left(1+2\frac{\varepsilon}{E_g}\right)^2}, \tag{B7}$$

$$\tau_{0,o}(T) = \frac{2\hbar^2 a^2 \rho(\hbar\omega_0)^2}{\pi E_{oc}^2 K_B T(2m_{d0})^{3/2}}, \tag{B8}$$

where a is the PbTe lattice constant, ρ is the PbTe density, ω_0 is the frequency of the optical phonons, K_o is the ratio of the optical deformation potential coupling constants for valance and conduction bands, $K_o=E_{ov}/E_{oc}$, which are taken to be the same as for the acoustic phonons, K_a.

(iii) Polar scattering by optical phonons (τ_{po}),

$$\tau_{po} = \frac{\left(\varepsilon+\frac{\varepsilon^2}{E_g}\right)^{1/2}F^{-1}}{e^2(2m_{d0})^{1/2}K_B T(\epsilon_\infty^{-1}-\epsilon_0^{-1})\left(1+2\frac{\varepsilon}{E_g}\right)}, \tag{B9}$$

$$F = 1-\delta\ln(1+\delta^{-1}) - \frac{2\frac{\varepsilon}{E_g}\left(1+\frac{\varepsilon}{E_g}\right)}{\left(1+2\frac{\varepsilon}{E_g}\right)^2}[1-2\delta+2\delta^2\ln(1+\delta^{-1})], \tag{B10}$$

$$\delta = (2kr_0)^{-2}, \tag{B11}$$

where ϵ_0 and ϵ_∞ are the static and high frequency dielectric constants, k is the carrier wave vector, and r_0 is the screening length of the optical phonons. The parameters k and r_0 are given by

$$k^2 = \frac{2m_{d0}\left(\varepsilon+\frac{\varepsilon^2}{E_g}\right)}{\hbar^2}, \tag{B12}$$

$$r_0^{-2} = \frac{2^{3/2}e^2 m_d^{3/2}}{\pi\hbar^3\epsilon_\infty}({}^0L_1^{1/2}), \tag{B13}$$

where ${}^nL_l^m$ is the generalized Fermi integral

$${}^nL_l^m(\mu,E_g) = \int_0^\infty \left(\frac{\partial f}{\partial\varepsilon}\right)\varepsilon^n\left[\varepsilon\left(1+\frac{\varepsilon}{E_g}\right)\right]^m\left(1+\frac{2\varepsilon}{E_g}\right)^l d\varepsilon. \tag{B14}$$

(iv) Short range deformation potential of vacancies (τ_v),

$$\tau_v = \frac{\tau_{0,v}(T)\left(\varepsilon+\frac{\varepsilon^2}{E_g}\right)^{-1/2}}{\left(1+2\frac{\varepsilon}{E_g}\right)[(1-A)^2-B]}, \tag{B15}$$

$$A = \frac{\frac{\varepsilon}{E_g}(1-K_v)}{\left(1+2\frac{\varepsilon}{E_g}\right)}, \tag{B16}$$

$$B = \frac{8\frac{\varepsilon}{E_g}\left(1+\frac{\varepsilon}{E_g}\right)K_v}{3\left(1+2\frac{\varepsilon}{E_g}\right)^2}, \tag{B17}$$

$$\tau_{0,v}(T) = \frac{\pi\hbar^4}{U_{vc}^2 m_{d0}(2m_{d0})^{1/2}N_v}, \tag{B18}$$

where N_v is the vacancy density, K_v is the ratio of the short range deformation potential coupling constants of vacancies for valence and conduction bands, $K_v=U_{vv}/U_{vc}$ which are taken to be the same as for acoustic phonons, K_a.

(v) Coulomb potential of vacancies (τ_C),

$$\tau_C = \frac{\epsilon_0^2(2m_{d0})^{1/2}\left(\varepsilon+\frac{\varepsilon^2}{E_g}\right)^{3/2}}{\pi(Ze^2)^2 N_v[\ln(1+\xi)-\xi/(1+\xi)]\left(1+2\frac{\varepsilon}{E_g}\right)}, \tag{B19}$$

$$\xi = (2kr_v)^{-2}, \tag{B20}$$

where Ze is the vacancy charge, and r_v is the screening radius of the vacancy potential given by

$$r_v^{-2} = \frac{4\pi e^2}{\epsilon_0}D(\mu), \tag{B21}$$

$$D(\mu) = \frac{2^{1/2}(m_{d0})^{3/2}}{\pi^2\hbar^3}\left(\mu-\frac{\mu}{E_g}\right)^{1/2}\left(1+2\frac{\mu}{E_g}\right), \tag{B22}$$

$D(\mu)$ being the density of states at the chemical potential.

[1] P. Zhu, Y. Imai, Y. Isoda, Y. Shinohara, X. Jia, and G. Zou, J. Phys.: Condens. Matter **17**, 7319 (2005).
[2] G. S. Nolas, J. W. Sharp, and H. J. Goldsmid, *Thermoelectrics: Basics Principles and New Materials Developments* (Springer-Verlag, Heidelberg, 2001).
[3] G. A. Slack, in *Thermoelectric Materials-New Directions and Approaches*, edited by T. M. Tritt, G. D. Mahan, H. B. Lyon, Jr., and M. G. Kanatzidis, MRS Symposia Proceedings No. 478 (Materials Research Society, Pittsburgh, PA, 1997), pp. 47–54.
[4] H. J. Goldsmid and A. W. Penn, Phys. Lett. A **27**, 523 (1968).
[5] P. G. Klemens, in *Modern Perspectives On Thermoelectrics and Related Materials*, edited by D. D. Alred, C. B. Vining, and G. A. Slack (Materials Research Society, Pittsburgh, PA, 1991), p. 87.
[6] L. D. Hicks and M. S. Desselhaus, Phys. Rev. B **47**, 12727(1993).
[7] J. O. Sofo and G. D. Mahan, Phys. Rev. B **49**, 4565 (1994).
[8] G. L. Bennett, in *CRC Handbook of Thermoelectrics*, edited by D. M. Rowe (CRC Press, New York, 1995), pp. 515–537.
[9] K. Kishimoto and T. Koyanagi, J. Appl. Phys. **92**, 2544 (2002).
[10] G. D. Mahan, Solid State Phys. **51**, 81 (1997).
[11] D. Bilc, S. D. Mahanti, E. Quarez, K.-F. Hsu, R. Pcionek, and M. G. Kanatzidis, Phys. Rev. Lett. **93**, 146403 (2004).
[12] T. C. Harman, D. L. Sprears, and M. J. Manfra, J. Electron. Mater. **25**, 1121 (1996); T. C. Harman, P. J. Taylor, M. P. Walsh, and B. E. LaForge, Science **297**, 2229 (2002).
[13] J. P. Heremans, C. M. Thrush, and D. T. Morelli, Phys. Rev. B **70**, 115334 (2004).
[14] J. R. Sootsman, H. Kong, C. Uher, A. Downey, J. James, D. Angelo, C. Wu, T. P. Hogan, T. Caillat, and M. G. Kanatzidis (unpublished).
[15] D. I. Bilc, S. D. Mahanti, and M. G. Kanatzidis, Phys. Rev. B **74**, 125202 (2006).
[16] C. M. Bhandari and D. M. Rowe, J. Phys. D **18**, 873 (1985).
[17] M. P. Singh and C. M. Bhandari, Pramana, J. Phys. **62**, 1309 (2004).
[18] D. M. Zayachuk, Semiconductors **31**, 173 (1997).
[19] D. M. Freik, L. I. Nykyruy, and V. M. Shperun, Semicond. Phys., Quantum Electron. Optoelectron. **5**, 362 (2002).
[20] J. M. Ziman, *Principles of the Theory of Solids* (Cambridge University Press, New York, 1964), p. 179.
[21] E. O. Kane, in *Semiconductors and Semimetals*, edited by R. K. Willardson and A. C. Beer (Academic, New York, 1975), Vol. 1, Chap. 3.
[22] Yu. I. Ravich, B. A. Efimova, and V. I. Tamarchenko, Phys. Status Solidi B **43**, 11 (1971).
[23] Yu. I. Ravich, B. A. Efimova, and I. A. Smirnov, *Semiconducting Lead Chalcogenides* (Plenum, New York, 1970), Vol. 5, p. 299.
[24] Y. W. Tsang and M. L. Cohen, Phys. Rev. B **3**, 1254 (1971).
[25] H. Yokoi, S. Takeyama, N. Miura, and G. Bauer, Phys. Rev. B **44**, 6519 (1991).
[26] G. D. Mahan and J. O. Sofo, Proc. Natl. Acad. Sci. U.S.A. **93**, 7436 (1996).
[27] E. Humphrey and H. Linke, Phys. Rev. Lett. **94**, 096601 (2005).
[28] B. A. Efimova, L. A. Kolomoets, Yu. I. Ravich, and T. S. Stavitskaya, Sov. Phys. Semicond. **4**, 1653 (1971).
[29] J. R. Drabble and H. J. Goldsmid, *International Series of Monographs on Semicondoctors: Thermal Conduction in Semiconductors* (Pergamon, New York, 1961), Vol. 4.